



**Fundació**  
La Marató de TV3  
XVI SIMPOSIUM  
Rare diseases

## Understanding and combating Duchenne muscular dystrophy progression in animal models

**Dr Eusebio Perdiguero Santamaria**

Faculty of Health and Life Sciences.  
Universitat Pompeu Fabra (UPF), Barcelona



## 1. Abstract

Duchenne muscular dystrophy (DMD), caused by defects in the dystrophin gene, is a rare neuromuscular disease affecting 1:3.300 boys. Muscle inflammation, necrosis and fibrosis occur as direct or indirect consequences of dystrophin deficiency so that DMD patients experience severe and progressive loss of muscle mass and function leading to death. Muscle stem cell (satellite cell) therapy has failed due to limited proliferation and survival of transplanted cells; however, transplantation of mesoangioblasts (stem cells from vascular mesodermal origin) has produced encouraging results in mice and dogs (pre-clinical model of DMD). Any cell-based therapeutic approach for DMD will require modification of the host fibrotic environment, based on its negative effects on stem cells functions and engraftment. Therefore, modifying the endogenous muscle stem cell and mesoangioblast properties, combined with reduction of host tissue fibrosis, may improve stem cell engraftment in DMD.

### **Background and hypothesis**

One critical regulator of muscle stem cell functions is the p38 MAPK pathway; however, whether modifications of p38 activity can influence muscle regeneration and stem cell engraftment in dystrophic muscle has never been explored. In this project we wanted to use mouse animal models of DMD (mdx mice) and genetically modified mice deficient in p38 $\alpha$  to investigate the function of this kinase in satellite cells and inflammatory cells' behavior during dystrophic muscle regeneration. Satellite cells and mesoangioblasts derived from wild type and p38 $\alpha$ -deficient mice would be transplanted into immune-deficient mdx mice (treated or not with anti-inflammatory/fibrotic agents) and their engraftment capacity into the dystrophic muscle would be subsequently analyzed.

### **Specific aims and work plan**

- To investigate the effects of p38 $\alpha$  deficiency in the evolution of the pathology in dystrophic muscle. To this end, we have generated conditional mouse models with muscle-specific deletion of p38 $\alpha$  in satellite cells, myofibers and macrophages, which will have crossed with the dystrophic (mdx) mice.
- To investigate comparatively the engraftment capacity of WT and p38 $\alpha$ -deficient satellite cells (which have shown enhanced proliferation and survival capacities in vitro) after transplantation in immune-deficient mouse models for muscular dystrophy (mdx/SCID).

- To study the engraftment capacity of fetal WT and p38 $\alpha$ -deficient cells in immune-deficient mouse models for muscular dystrophy.
- To investigate the influence of an optimized host environment (by pharmacological anti-inflammatory and antifibrotic treatment), combined with specific p38 $\alpha$  deletion in satellite cells and mesoangioblasts, in enhancing the engraftment potential of these cell types in dystrophic mice.

## 2. Results

### **p38 $\alpha$ in mdx dystrophy progression**

#### **Generation of mdx/Pax7-CRE/p38 $\alpha$ (mdx/Mgn-CRE/p38 $\alpha$ ) and mdx/Lys-CRE/p38 $\alpha$ double-mutant mice.**

p38 $\alpha$  null mice are embryonic lethal (Adams et al., 2000). We generated conditional mutant mice that lacked p38 $\alpha$  in skeletal muscle by disrupting the p38 $\alpha$  gene in the Pax7 or Myogenin progeny and that lacked p38 $\alpha$  in the myeloid compartment by disrupting the p38 $\alpha$  gene in the Lysozyme2 (Lyz2) progeny using the Cre/loxP system (Clausen et al., 1999). p38 $\alpha^{\Delta Pax7}$ , p38 $\alpha^{\Delta Myog}$  and p38 $\alpha^{\Delta LySM}$  mice were born with the expected Mendelian ratios and had lifespans comparable to their wild type (p38 $\alpha^{WT}$ ) littermates. To analyze the role of p38 $\alpha$  in mdx muscle regeneration, mdx mice were crossed with p38 $\alpha^{\Delta Pax7}$ , p38 $\alpha^{\Delta Myog}$  and p38 $\alpha^{\Delta LySM}$  mice respectively. Double-mutant mice downregulated p38 $\alpha$  levels in all the skeletal muscles analyzed as well as in the diaphragm, while no changes were observed in the heart, liver, or white adipose tissues (**Fig. 1A**). To characterize double-mutant mice in the myeloid lineage we isolated macrophages from 3-month old mdx and mdx/p38 $\alpha^{\Delta LySM}$  mice in vivo using a well-established FACS sorting technique (Perdiguero et al., 2011) (**Fig. 1B**) and demonstrated that p38 $\alpha$  levels were downregulated in the myeloid compartment, to a 90% (**Fig. 1C**). We did not observe any differences between mdx/p38 $\alpha^{\Delta Pax7}$  and mdx/p38 $\alpha^{\Delta Myog}$  so in all further analysis we used mdx/p38 $\alpha^{\Delta Pax7}$ .

## **Analysis of the consequences of p38 $\alpha$ deficiency in mdx muscle regeneration.**

### **p38 $\alpha$ deficiency in muscle cells**

mdx and double mutant mdx/p38 $\alpha^{\Delta Pax7}$  mice were healthy at birth and did not show any signs of muscle injury or differences in muscle size before disease onset (14 d of age). p38 $\alpha^{\Delta Pax7}$  mice have smaller muscles (Brien et al., 2013) and accordingly the mdx/p38 $\alpha^{\Delta Pax7}$  mice presented reduced body weight at 3 or 12 months (**Fig. 1D**). Regarding muscle, first we analyzed mice at 3 months of age, at the onset of the disease. Compared with mdx mice, mdx/p38 $\alpha^{\Delta Pax7}$  mice had slightly increased levels of dystrophinopathy as characterized by the size of central nucleated myofibers (regenerating fibers) (**Fig. 1D**), where muscles contained more clusters of early regenerating myofibers (**Fig. 1E**) both in limb muscles and in diaphragm (data not shown). To ascertain whether these differences would cause a functional reduction in muscle performance, we did an exercise tolerance test, where muscle strength at 3 months of age was similar in both genotypes (data not shown). We wanted then to know whether this phenotype increased with age, when dystrophic muscle function is further compromised by accumulation of inflammation and fibrosis. Since it has been demonstrated in several studies that in the mdx mouse model regeneration capacity is reduced and muscle wasting in the diaphragm muscle is more severe than in the hind limb, we analyzed the status of diaphragm muscle in mdx and mdx/p38 $\alpha^{\Delta Pax7}$  mice of 12 months of age. Compared with mdx mice, mdx/p38 $\alpha^{\Delta Pax7}$  mice at 12 months have no significant difference in their levels of dystrophinopathy as characterized by the size of central nucleated myofibers (regenerating fibers) (**Fig. 2A**), but with a 30 % reduction in the numbers of early/medium/late regenerating myofibers in the diaphragm. In agreement with the reduction in fiber number, the amount of fibrotic tissue increased in the mdx/p38 $\alpha^{\Delta Pax7}$  diaphragm, as indicated by the amount of collagen deposition stained by Sirius Red. To ascertain whether these differences would cause an increase in muscle damage or a functional reduction in muscle performance, we determined the levels of creatine kinase (CK) in serum, both in resting muscle and after performing an exercise tolerance test. Systemic muscle damage and muscle strength were similar in both genotypes (**Fig. 2B, 2C**). Altogether, these results indicate histological, biochemical, and functional evidence that p38 $\alpha$  deficiency aggravates the onset of the disease in young mice but that at later stages of the dystrophinopathy p38-deficiency does

not have increasing impact in the evolution of the disease. Preliminary results with older mice (near 2 years of age) indicate that p38-deficiency could be beneficial in aged animals.

### **p38 $\alpha$ in stem cell engraftment in dystrophic muscle**

One of the major problems of cell therapies for muscular dystrophies has classically been the poor engraftment capacity of muscle stem cells (satellite cells). Therefore, vascular progenitors with capacity to form muscle upon transplantation have been used by Dr. Giulio Cossu's group as an alternative for engraftment in dystrophic muscle. However, in the context of the Optistem EU network (where the UPF Cell Biology unit is a member), the human clinical trial for DMD directed by our collaborator at the San Raffaele Hospital (Milan, Italy) using mesoangioblasts, despite offering positive and encouraging outcomes, has evidenced the need not only of improving the host muscle environment but also of reanalyzing the cells to be transplanted (Tedesco F.S. and Cossu G. personal communication). Indeed, mesoangioblasts have a vascular/pericyte origin, and given their plastic nature, pericytes have recently been shown to give rise to muscle, but under conditions of damage they can also transdifferentiate into fibrogenic cells, thereby promoting undesirable fibrosis (Dulauroy et al., 2012). Thus, we rethought our strategy and, based on the considerations explained above, we devoted great effort to improving the engraftment of the bona fide muscle stem cells, the satellite cells and abandoned Task 3. In that sense, we have set up new isolation and engraftment protocols following the advice of leading experts in our field (Rocheteau et al., 2012). Following this strategy we have analyzed potential factors by which satellite cells, and especially satellite cells from mdx mice, have a regenerative decline and display poor engraftment capacity, before analyzing the role of p38 $\alpha$ . First, we analyzed the number of satellite cells in muscle of mdx mice and compared it to age-matched wild type (WT) mice. Using single fiber explants, we found that the number of satellite cells per myofiber (identified by Pax7 expression) was similar in young WT and mdx mice of 2 months of age (**Fig. 2D, 2E**). Importantly, we found that the expression of p16<sup>INK4a</sup> (a tumor suppressor and cell cycle inhibitor) was undetectable in satellite cells from both WT and mdx mice at young age, as shown by RT-qPCR analysis of FACS isolated satellite cells (**Fig. 4c**). We found, however, that the number of satellite cells declined rapidly with age in mdx mice, as disease progressed (**Fig. 2E**). Indeed, the number of satellite cells in muscle of adult mdx mice of 9

months of age was low compared to age-matched adult WT mice, suggesting that the continuous degeneration/regeneration cycles in the dystrophic muscle were affecting satellite cell number. Very interestingly, we found that, while satellite cells from WT mice of 9 months of age did not express p16<sup>INK4a</sup> (as expected), satellite cells from mdx mice did express p16<sup>INK4a</sup> at the same age (**Fig. 2F**). These findings suggested that de-repression of p16<sup>INK4a</sup> in satellite cells from mdx mice with aging may exacerbate their myogenic defect for engraftment.

To investigate the effect of anticipated p16<sup>INK4a</sup> expression in satellite cells in vivo, we used Bmi1-deficient (Bmi1<sup>-/-</sup>) mice (a member of Polycomb repressive complex 1 PRC1 which is widely known to repress p16<sup>INK4a</sup> expression). As expected, p16<sup>INK4a</sup> was de-repressed in Bmi1-deficient satellite cells from young/adult (**Fig. 3A**). Importantly, elevated p16<sup>INK4a</sup> expression correlated with the impaired activation of Bmi1-deficient quiescent satellite cells, and defective regenerative capacity of Bmi1 null muscle after injury (**Fig. 3B**). Furthermore, FACS purified transplanted Bmi1<sup>-/-</sup> satellite cells overexpressing p16<sup>INK4a</sup> exhibited a low activation rate from quiescence after damage and contributed poorly to the formation of new myofibers within muscles of immunodeficient WT muscle hosts compared to Bmi1<sup>+/+</sup> satellite cells (**Fig. 3C**). These results indicate that satellite cells from Bmi1 null mice have a poor engraftment capacity, which is likely attributable to the induction of p16<sup>INK4a</sup>. To prove the causal role of p16<sup>INK4a</sup> in the cell-intrinsic defective regenerative capacity of Bmi1 null satellite cells, p16<sup>INK4a</sup> was silenced in freshly sorted Bmi1 null satellite cells prior to engraftment into muscle of immunodeficient mice, followed by injury (**Fig. 3D**). We found that loss of p16<sup>INK4a</sup> sufficed to restore activation in engrafted Bmi1 null satellite cells (**Fig 3E, 3F**). In summary, we have identified p16<sup>INK4a</sup> as a factor whose induced expression in resting satellite cells impairs their subsequent engraftment. Notably, we have found p16<sup>INK4a</sup> is upregulated in satellite cells from aging mice, correlating with the decline in muscle regeneration associated to aging (Sousa-Victor et al., 2014) (results not shown). Importantly, silencing of p16<sup>INK4a</sup> also restored endogenous regeneration of aging mice and the regenerative potential of aged satellite cells overexpressing p16<sup>INK4a</sup> in cell transplantation experiments (Sousa-Victor et al., 2014). Taken together, since satellite cells of adult mdx mice overexpress p16<sup>INK4a</sup> and display a very poor engraftment capacity and regenerative potential, we propose that downregulating p16<sup>INK4a</sup> expression could improve satellite cell therapy for DMD.

### **Analysis of the role of p38 $\alpha$ in satellite cell engraftment in dystrophic mice.**

#### **Analysis of the engraftment of wild type and p38 $\alpha$ -deficient satellite cells in immunodeficient mdx/SCID or $\alpha$ -sarcoglycan/SCID mice.**

Following the strategy explained above, satellite cells were isolated from wild type or p38 $\alpha$ .<sup>Pax7</sup> mice, and injected into mdx/SCID mice. Mice were analyzed 21 days after injection and the functional recovery of the dystrophic muscles was analyzed measuring parameters indicative of muscular degeneration/regeneration, and the de novo expression of dystrophin. As we have demonstrated for young, adult and aged satellite cells (Sousa-Victor et al., 2014), p38 $\alpha$ -deficient satellite cells were able to engraft into mdx muscles and allow formation of new fibers which expressed dystrophin (**Fig. 3G**). Despite this success, our current data do not show any significant difference in the efficiency of engraftment between WT and p38 $\alpha$ .<sup>Pax7</sup> satellite cells. Since p38 $\alpha$ -deficient satellite cells have a quite different expression profile (Brien et al., 2013 and our own unpublished data) and functional properties in vitro (Brien et al., 2013; Perdiguero et al., 2011; Ruiz-Bonilla et al., 2008) we are quite puzzled by these results. Since we did these experiments with young (2-3 months) mice and taking into account our data linking muscular dystrophy with p16<sup>INK4a</sup> expression and the body of evidence linking p38 signaling pathway with the induction of senescence, we are now doing experiments with adult (6 months) or aged mdx and mdx/p38 $\alpha$ .<sup>Pax7</sup> satellite cells trying to see whether p38 pathway could control the drop in performance of satellite cell occurring during the evolution of muscular dystrophy disease over time.

### **Influence of the host environment on stem cell engraftment.**

#### **Analysis of the role of macrophages produced p38 $\alpha$ on the reduction of inflammation and fibrosis in dystrophic muscle.**

First we analyzed macrophages from WT and p38 $\alpha$ . <sup>$\Delta$ LysM</sup> mice isolated from an acute injury model. To do so we have set up a new protocol of separation of neutrophils and the different macrophage subpopulations in injured muscle which go one step further than our previous strategy (Perdiguero et al., 2011) and allow us to separate neutrophils (F4/80<sup>-</sup> Ly6C<sup>High</sup>), M1 proinflammatory macrophages (F4/80<sup>+</sup> Ly6C<sup>High</sup>) and two populations of M2 anti-inflammatory macrophages F4/80<sup>+</sup> Ly6C<sup>Low</sup> MHCII<sup>High</sup> (M2b like) or MHCII<sup>Low</sup> (M2c) (**Fig. 4A**). With this new gating strategy we have discovered that p38 $\alpha$  loss induces a switch in the expression of IL-1 $\beta$  and IL-10 cytokines expressed specifically in the M2c

F4/80<sup>+</sup> Ly6C<sup>Low</sup> MHCII<sup>Low</sup> population of macrophages at 6 days post-injury (**Fig. 4B**), a stage of the chronic injury which is most similar to the mdx mice inflammatory status (**Fig. 4C**). With this information, we then undertook the analysis of the mdx and double mutant mdx/p38 $\alpha^{\Delta\text{LysM}}$  mice at the onset of the dystrophinopathy (3 months). mdx/p38 $\alpha^{\Delta\text{LysM}}$  mice have no obvious differences in body weight and global size of limb muscles so we analyzed diaphragm muscle. mdx/p38 $\alpha^{\Delta\text{LysM}}$  mice did not show significant differences in the size of central nucleated myofibers (regenerating fibers) and in fibrotic area compared with mdx mice (**Fig. 4D**). Since we encountered serious breeding problems with this colony, we are currently accumulating bigger cohorts of animals to ascertain these results and also to do functional studies.

#### **Analysis of the consequences of reducing inflammation and fibrosis in the host dystrophic muscle on stem cell engraftment.**

##### **Effect of anti-miR-21-induced reduction of inflammation and fibrosis of mdx mice on the engraftment of satellite cells.**

We have characterized a new age-associated fibrogenic regulatory axis in the dystrophic mouse model. The expression of miR-21, which is barely detected in normal muscle, increased concomitantly with age-dependent fibrogenesis. Modulation of miR-21 in muscles of aged dystrophic mice by treatment with a miR-21 inhibitor (Ant-miR-21) reversed fibrosis in limb muscles at stage at which mdx fibrosis is generally considered irreversible (**Fig. 5A, 5B**) (Ardite et al., 2012). In order to analyze the influence of the anti-miR-21 treatment on the engraftment of satellite cells into dystrophic muscle, we transplanted immunodeficient mdx control mice, or mice pretreated with miR-21 inhibitor (Ant-miR-21) to reduce inflammation and fibrosis development with  $5 \times 10^5$  satellite cells, mice previously transduced with a lentiviral vector expressing GFP, as described previously (**Fig. 5C**). We observed a significant increase in number of GFP<sup>+</sup> myofibers in Ant-miR-21 treated mdx mice versus untreated mdx mice, at 7 and 21 days after satellite cell injection (**Fig. 5C and unpublished data**), proving the beneficial effect of the anti-fibrotic treatment in the engraftment efficiency. Together with this engraftment improvement we observed a reduced fibrosis deposition, supporting our hypothesis that the antifibrotic effect of antago-miR-21 treatment improves both host tissue environment and stem cell engraftment.



## References

- Adams, R.H., A. Porras, G. Alonso, M. Jones, K. Vintersten, S. Panelli, A. Valladares, L. Perez, R. Klein, and A.R. Nebreda. 2000. Essential role of p38alpha MAP kinase in placental but not embryonic cardiovascular development. *Mol Cell*. 6:109-116.
- Ardite, E., E. Perdiguero, B. Vidal, S. Gutarra, A.L. Serrano, and P. Munoz-Canoves. 2012. PAI-1-regulated miR-21 defines a novel age-associated fibrogenic pathway in muscular dystrophy. *The Journal of cell biology*. 196:163-175.
- Brien, P., D. Pugazhendhi, S. Woodhouse, D. Oxley, and J.M. Pell. 2013. p38alpha MAPK regulates adult muscle stem cell fate by restricting progenitor proliferation during postnatal growth and repair. *Stem Cells*. 31:1597-1610.
- Clausen, B.E., C. Burkhardt, W. Reith, R. Renkawitz, and I. Forster. 1999. Conditional gene targeting in macrophages and granulocytes using LysMcre mice. *Transgenic research*. 8:265-277.
- Dulauroy, S., S.E. Di Carlo, F. Langa, G. Eberl, and L. Peduto. 2012. Lineage tracing and genetic ablation of ADAM12(+) perivascular cells identify a major source of profibrotic cells during acute tissue injury. *Nat Med*.
- Gunther, S., J. Kim, S. Kostin, C. Lepper, C.M. Fan, and T. Braun. 2013. Myf5-positive satellite cells contribute to Pax7-dependent long-term maintenance of adult muscle stem cells. *Cell Stem Cell*. 13:590-601.
- Lepper, C., S.J. Conway, and C.M. Fan. 2009. Adult satellite cells and embryonic muscle progenitors have distinct genetic requirements. *Nature*. 460:627-631.
- Palacios, D., C. Mozzetta, S. Consalvi, G. Caretti, V. Saccone, V. Proserpio, V.E. Marquez, S. Valente, A. Mai, S.V. Forcales, V. Sartorelli, and P.L. Puri. 2010. TNF/p38alpha/polycomb signaling to Pax7 locus in satellite cells links inflammation to the epigenetic control of muscle regeneration. *Cell Stem Cell*. 7:455-469.

Perdiguero, E., P. Sousa-Victor, V. Ruiz-Bonilla, M. Jardi, C. Caelles, A.L. Serrano, and P. Munoz-Canoves. 2011. p38/MKP-1-regulated AKT coordinates macrophage transitions and resolution of inflammation during tissue repair. *The Journal of cell biology*. 195:307-322.

Rocheteau, P., B. Gayraud-Morel, I. Siegl-Cachedenier, M.A. Blasco, and S. Tajbakhsh. 2012. A subpopulation of adult skeletal muscle stem cells retains all template DNA strands after cell division. *Cell*. 148:112-125.

Ruiz-Bonilla, V., E. Perdiguero, L. Gresh, A.L. Serrano, M. Zamora, P. Sousa-Victor, M. Jardi, E.F. Wagner, and P. Munoz-Canoves. 2008. Efficient adult skeletal muscle regeneration in mice deficient in p38beta, p38gamma and p38delta MAP kinases. *Cell Cycle*. 7:2208-2214.

Sousa-Victor, P., S. Gutarra, L. Garcia-Prat, J. Rodriguez-Ubreva, L. Ortet, V. Ruiz-Bonilla, M. Jardi, E. Ballestar, S. Gonzalez, A.L. Serrano, E. Perdiguero, and P. Munoz-Canoves. 2014. Geriatric muscle stem cells switch reversible quiescence into senescence. *Nature*.

### 3. Relevance and implications

During the realization of this project we have learned that combination therapies for treatment of DMD is not only a promising idea but the only feasible possibility for a cure. The hope for an “easy” method of transplantation of vascular-derived cells that will reach and engraft the muscle after systemic administration has been demonstrated to be more difficult than expected with very modest results in the clinical trial that has been performed in the context of Optistem European FP7 project. Perhaps this trial could have been more successful if combined with an anti-inflammatory and antifibrotic treatment, though worrying news on mesoangioblast has been published as mentioned above. Therefore we have concentrated our attention on satellite cells, since new advances in satellite cell isolation and engraftment techniques have made it possible to use them in proof of principle studies. As for the p38 MAPK signaling pathway, our results highlight that the role of this kinase is more complicated than expected. p38 $\alpha/\beta$  has been reported to repress

Pax7 expression by activating the Polycomb repressive complex 2 (PRC2) (Palacios et al., 2010). One could hypothesize that, in vivo, ablation of p38 $\alpha$  may cause a persistent expression of Pax7 in myoblasts, leading to increased proliferation and reduced differentiation. Strikingly, however, contrary to our previous in vitro data, we did not observe that deletion of p38 $\alpha$  in adult satellite cells did not affect proliferation although it was important for proper satellite cell activation (Zamora et al., in preparation). This suggests that the axis p38 $\alpha$ -Pax7 may apply to myoblast differentiation but does not play an active role in adult satellite cells, at least not in differentiation. Furthermore, it has been demonstrated that there is a cell-intrinsic difference in the Pax7 dependency between neonatal and adult satellite cells, based on which they proposed that the function of satellite cells has age-dependent genetic requirements (Gunther et al., 2013; Lepper et al., 2009). Our current data suggest that p38a is one of the important molecules for defining the age-dependent behavior of satellite cells, a topic that we continue investigating both in WT mice and dystrophic mice. Therefore our initial idea that p38 inhibition might be beneficial in the treatment of the onset of dystrophic disease might be true for later stages of the disease.

Regarding the use of stem cell engraftment and anti-inflammatory/antifibrotic drugs as a better treatment for Duchenne muscular dystrophy, we have demonstrated that a combination of miR-21 inhibition with satellite cell engraftment improves the efficiency of the transplant and moreover reduced fibrosis deposition, supporting our hypothesis that the antifibrotic effect of miR-21 inhibition will improve both host tissue environment and stem cell engraftment.

#### 4. Literature generated

Ardite E, Perdiguero E, Vidal B, Gutarra S, Serrano AL, Muñoz-Cánoves P. PAI-1-regulated miR-21 defines a novel age-associated fibrogenic pathway in muscular dystrophy. *J Cell Biol.* 2012 196(1):163-75.

Muñoz-Cánoves P, Scheele C, Pedersen BK, Serrano AL. Interleukin-6 myokine signaling in skeletal muscle: a double-edged sword? *FEBS J.* 2013 Sep;280(17):4131-48. doi: 10.1111/febs.12338. Corresponding author

Kharraz Y, Guerra J, Mann CJ, Serrano AL, Muñoz-Cánoves P. Macrophage plasticity and the role of inflammation in skeletal muscle repair. *Mediators Inflamm.* 2013;2013:491497. doi: 10.1155/2013/491497. Corresponding authors

Sousa-Victor P, Gutarra S, García-Prat L, Rodríguez-Ubreva J, Ortet L, Ruiz-Bonilla V, Jardí M, Ballestar E, González S, Serrano AL, *Perdiguero E, Muñoz-Cánoves P.* Geriatric muscle stem cells switch reversible quiescence into senescence. *Nature.* 2014 Feb 12. doi: 10.1038/nature13013. Corresponding authors

Perdiguero E, Sousa-Victor P, Ruiz-Bonilla V, Jardí M, Caelles C, Serrano AL, Muñoz-Cánoves P. p38/MKP-1-regulated AKT coordinates macrophage transitions and resolution of inflammation during tissue repair. *J Cell Biol.* 2011 195(2):307-22.

Perdiguero E, Kharraz Y, Serrano AL, Muñoz-Cánoves P. MKP-1 coordinates ordered macrophage-phenotype transitions essential for stem cell-dependent tissue repair. *Cell Cycle.* 2012 11(5):877-86.

## Figures

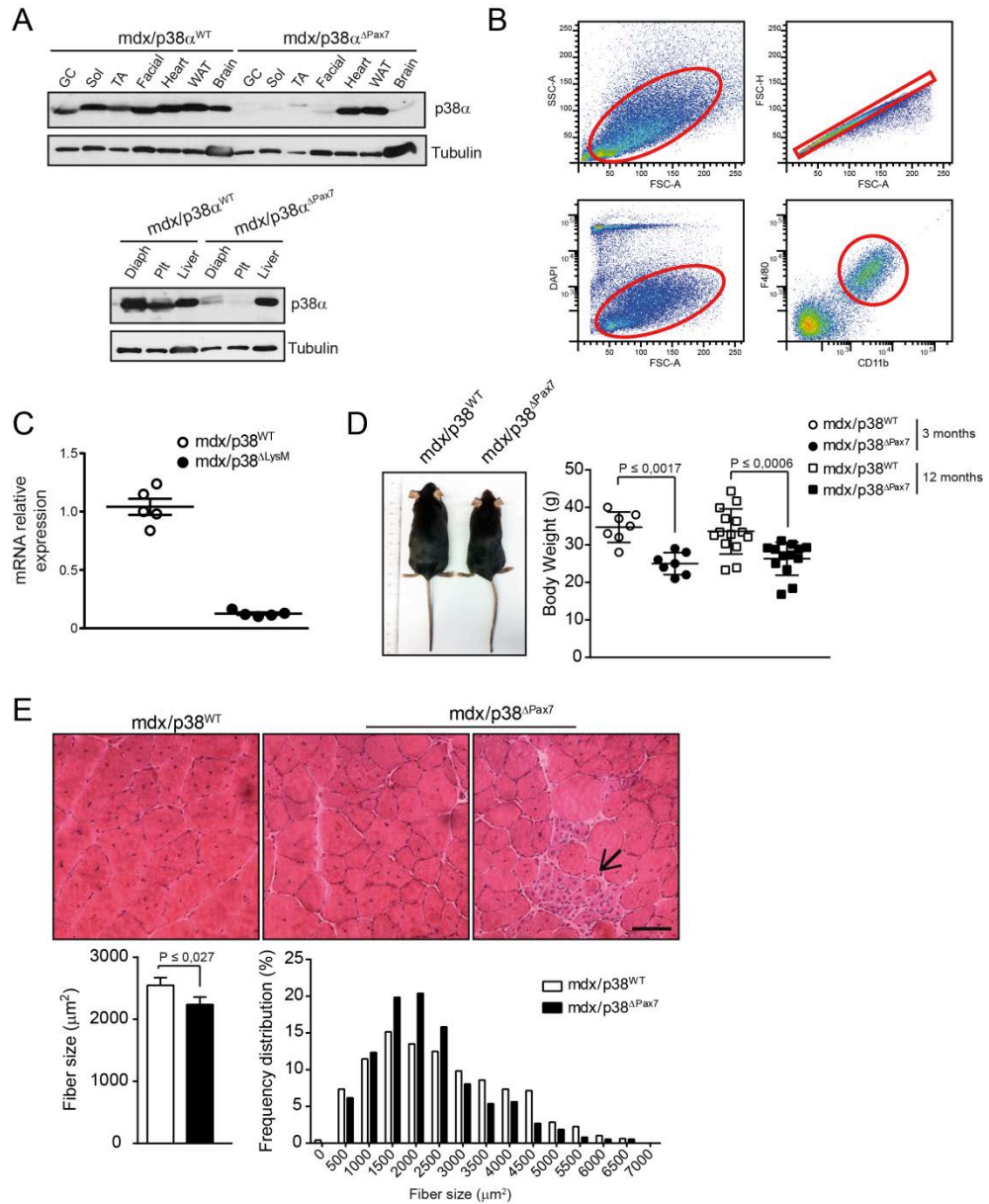


**Figure 1.** Efficiency and specificity of CRE mediated p38 $\alpha$  deletion and effect of p38 $\alpha$  deletion in dystrophic muscle cells at 3 months. **A.** Western blot analysis shows p38 $\alpha$  protein level in different tissues from mdx/ p38 $\alpha$ <sup>WT</sup> and mdx/p38 $\alpha$  <sup>$\Delta$ Pax7</sup>. GC: gastrocnemius, SOL: soleus, TA: tibialis anterior, WAT: white adipose tissue, Diaph: diaphragm, Plt: plantaris.  $\alpha$ -tubulin is used as loading control. Similar results were obtained for Myogenin-Cre-mediated mutant mice (mdx/p38 $\alpha$  <sup>$\Delta$ Myog</sup>) with the exception of brain tissue where p38

expression was as in mdx/ p38 $\alpha$ <sup>WT</sup> mice. **B.** FACS strategy for isolation of macrophages from mdx and mdx/p38 $\alpha$  <sup>$\Delta$ LysM</sup> skeletal muscles. Viable cells were identified based on forward/side scatter, DAPI staining to exclude anuclear debris and dead cells. F4/80 and CD11b double positivity defined the macrophage population. **C.** Relative mRNA levels of p38 $\alpha$  was evaluated by RT-qPCR from the sorted macrophages. **D.** Representative images of mdx and mdx/p38 $\alpha$  <sup>$\Delta$ Pax7</sup> mice at 3 months of age and quantification of body weight at 3 and 12 months of age. **E** (top) Representative images of Hematoxylin/Eosin staining in cryosections of tibialis anterior (TA) muscle from mdx and mdx/p38 $\alpha$  <sup>$\Delta$ Pax7</sup> mice at 3 months of age. Arrow points to a cluster of smaller early regenerating myofibers. Scale bar represents 50  $\mu$ m. (bottom) Quantification of mean fiber size from TA muscles and frequency distribution. Data show mean  $\pm$  s.e.m. Comparisons by two-sided Mann–Whitney U-test. P values are indicated. n  $\geq$  5.

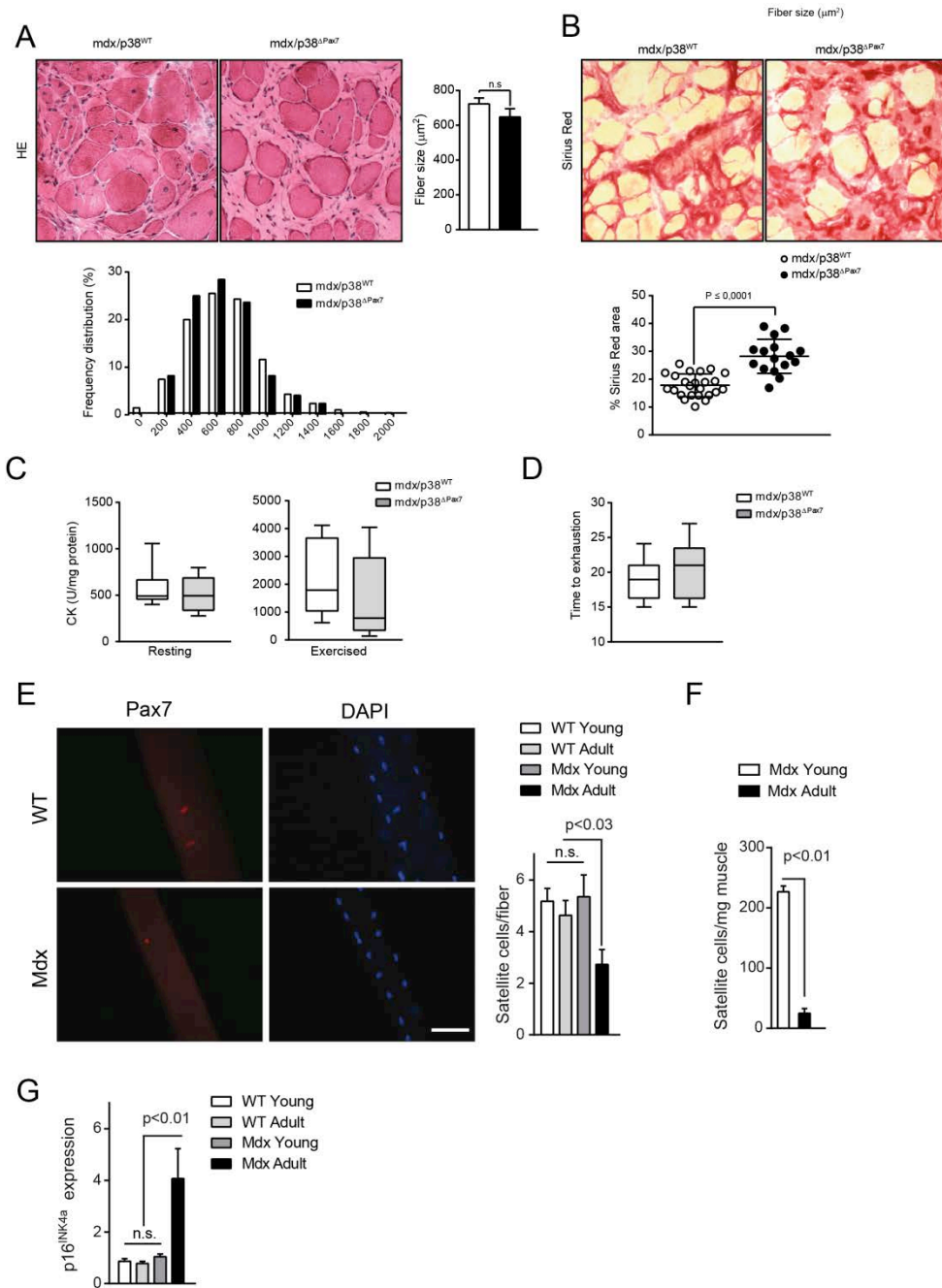


**Figure 2. A.** Representative images of Hematoxylin/Eosin staining in cryosections of diaphragm muscle from mdx and mdx/p38<sup>ΔPax7</sup> mice at 3 months of age and quantification of fiber size means (top). Frequency distribution of fiber cross-sectional area (bottom). **B.** Representative images of Sirius Red staining (as a measure to satin Collagen) in cryosections of diaphragm muscle from mdx and mdx/p38<sup>ΔPax7</sup> mice at 3 months of age

and quantification of Sirius Red stained area per sections (10 sections per muscle). **C.** Before sacrifice, mice from were assayed for Creatine Kinase activity in plasma (as a measure of muscle damage) from resting mice (left) prior to exercise (right) **D.** Mice ran to exhaustion on a treadmill. Bars depict mean values, and error bars represent SE. Comparisons by two-sided Mann–Whitney U-test. P values are indicated.  $n \geq 5$ . **E.** Single fiber explants of adult WT and mdx mice. Immunostaining of Pax7 satellite cells outside the myofiber are shown. DAPI staining to identify satellite cell nuclei and fiber myonuclei. The number of satellite cells (Pax7<sup>+</sup>) was quantified in single fiber explants of WT and mdx mice of distinct ages: young (2 months) and adult (9 months). The number of satellite cells is similar in WT and mdx mice of young age. In adult WT mice, the number of satellite cells remains constant. However, satellite cell number is reduced in adult mdx mice. **F.** Analysis of satellite cell number in FACS isolated satellite cells using a7-integrin/CD34 purification strategy. Confirming the results in single fiber extracts, FACS analysis shows that the number of satellite cells is reduced in muscle of adult versus young mdx mice. **G.** Analysis of p16<sup>INK4a</sup> expression in FACS isolated satellite cells of WT and mdx mice of distinct ages: young (2 months) and adult (9 months). WT satellite cells did not express p16INK4a at young or adult age. In contrast, the expression of p16INK4a was induced in adult satellite cells of mdx mice. Together, the results shown in a, b and c suggest that the loss of satellite cells in adult dystrophic mice might be related to the anticipated expression of p16<sup>INK4a</sup>. Thus, is tempting to propose that de-repression of p16<sup>INK4a</sup> in satellite cells from dystrophic muscle may exacerbate their myogenic defect and lead to their depletion during disease progression.



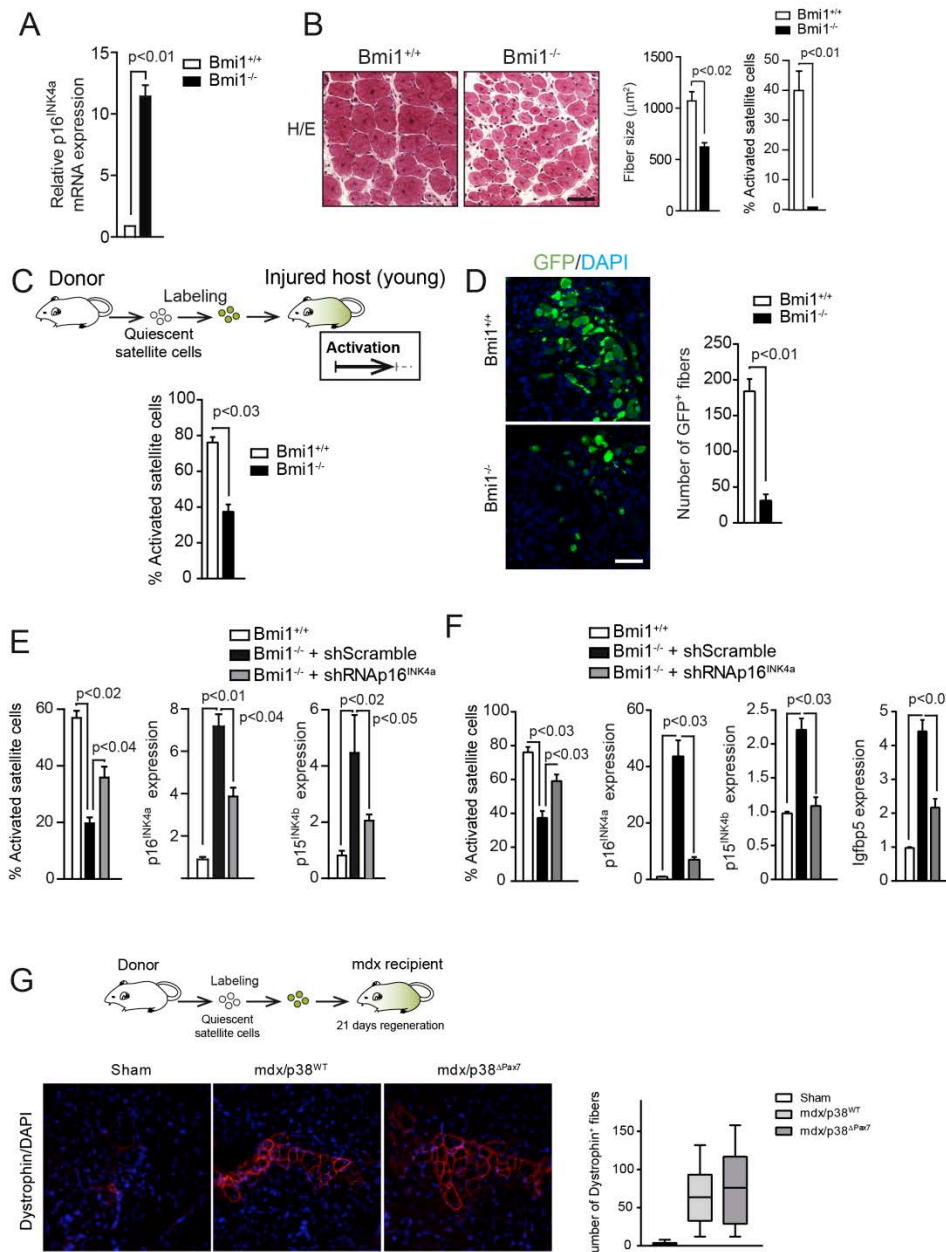


**Figure 3.** Engraftment capacity and regenerative potential is impaired in Bmi1 null satellite cells overexpressing p16<sup>INK4a</sup> after transplantation in a heterologous mouse host. p16<sup>INK4a</sup> silencing restores activation from quiescence in Bmi1 null satellite cells **A**. Expression of p16<sup>INK4a</sup>, evaluated by RT-qPCR, in

satellite cells isolated from young/adult Bmi1<sup>+/+</sup> and Bmi1<sup>-/-</sup> mice. **B**. Representative pictures of satellite cell-derived newly formed regenerating myofibers, stained with H/E in TA muscle cryosections of adult Bmi1<sup>+/+</sup> and Bmi1<sup>-/-</sup> mice injured by CTX injection and analyzed one week post injury. Histogram represents the quantification of regenerating myofiber size, evaluated by the cross-sectional area. (Right) Percentage of activated (Pax7/MyoD double positive) satellite cells in single fiber explants isolated from Bmi1<sup>+/+</sup> and Bmi1<sup>-/-</sup> mice. **C**, **D**. Scheme of transplantation assay of GFP-labeled satellite cells into

pre-injured immunodeficient WT mouse hosts. Equal numbers of FACS purified satellite cells from resting muscle of  $Bmi1^{+/+}$  and  $Bmi1^{-/-}$  mice were transplanted into muscles of immunodeficient WT mice, and activated satellite cells and new regenerating myofibers were analyzed at 24 hours and 7 days post-transplantation, respectively. **D.** Representative images of transplanted muscles after 7 days are shown. **E.** Equal numbers of satellite cells isolated by FACS from  $Bmi1^{+/+}$  and  $Bmi1^{-/-}$  mice were transduced with Ad-shRNAp16<sup>INK4a</sup> (expressing an shRNA specific for p16<sup>INK4a</sup>) or Ad-shScramble, and cultured in proliferative conditions. BrdU-positive cells were quantified before the first division, and p16<sup>INK4a</sup> and p15<sup>INK4b</sup> expression was determined by RT-qPCR. **F.** Equal numbers of satellite cells from resting muscle of  $Bmi1$  null mice, and their corresponding age-matched control mice, were isolated by FACS, p16<sup>INK4a</sup> silenced via liposome-mediated delivery of shRNAp16<sup>INK4a</sup> (or shScramble) and labeled with PKH26 dye, and immediately transplanted into pre-injured muscle of young mice; activation was analyzed 24 hours later by quantifying the number of sorted MyoD<sup>+</sup> or Ki67<sup>+</sup> satellite cells (results of MyoD<sup>+</sup> cells are shown); cell cycle inhibitors/senescence-associated markers including p16<sup>INK4a</sup>, p15<sup>INK4b</sup> and Igfbp5 were analyzed in sorted labeled cells by RT-qPCR. **G.** Engraftment of p38a-deficient satellite cells. Scheme of transplantation assay of GFP-labeled satellite cells into mdx mouse hosts. Equal numbers of satellite cells isolated by FACS from mdx and mdx/p38 $\alpha$ <sup>Pax7</sup> mice were transduced with GFP lentivirus and immediately transplanted into mdx mice. After 21 days, muscles were immunostained for dystrophin. The number of dystrophin<sup>+</sup> fibers per muscle is shown. Bars depict mean values, and error bars represent SE.

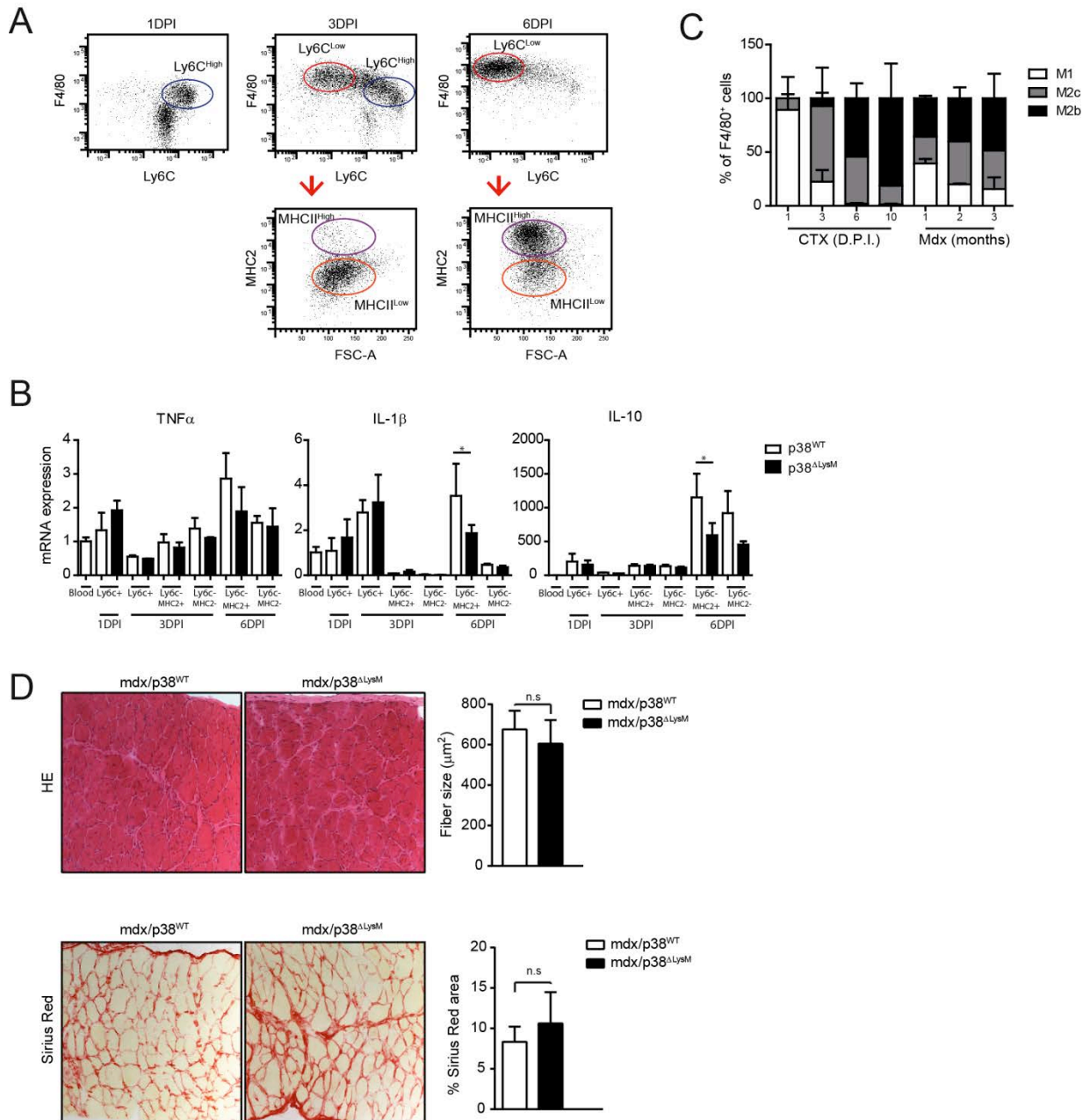


**Figure 4.** Cytokine expression in p38 $\alpha$ -deficient macrophages. **A.** FACS gating strategy to separate macrophage subpopulations in injured muscle at the indicated times post injury. **B.** Expression of indicated cytokines p38<sup>WT</sup> and p38 <sup>$\Delta$ LysM</sup> mice at the indicated times post injury. **C.** Comparison of the composition of the macrophage population between acute injury and chronic injury in the mdx mice at the indicated time points. Bars depict mean values, and error bars represent SE. Comparisons by two-sided Mann–Whitney U-test. P

value < 0.01. n ≥ 3. **D.** Effect of p38 $\alpha$  deletion in dystrophic macrophages at 12 months. (top) Representative images of Hematoxylin/Eosin staining in cryosections of diaphragm muscle from mdx and mdx/p38 $\alpha^{\Delta_{LysM}}$  mice at 3 months of age and quantification of fiber size means (top). (bottom) Representative images of SiriusRed staining (as a measure to stain collagen) in cryosections of diaphragm muscle from mdx and mdx/p38 $\alpha^{\Delta_{LysM}}$  mice at 3 months of age and quantification of Sirius Red stained area per sections (10 sections per muscle). Bars depict mean values, and error bars represent SE. Comparisons by two-sided Mann–Whitney U-test. P values are indicated. n ≥ 5

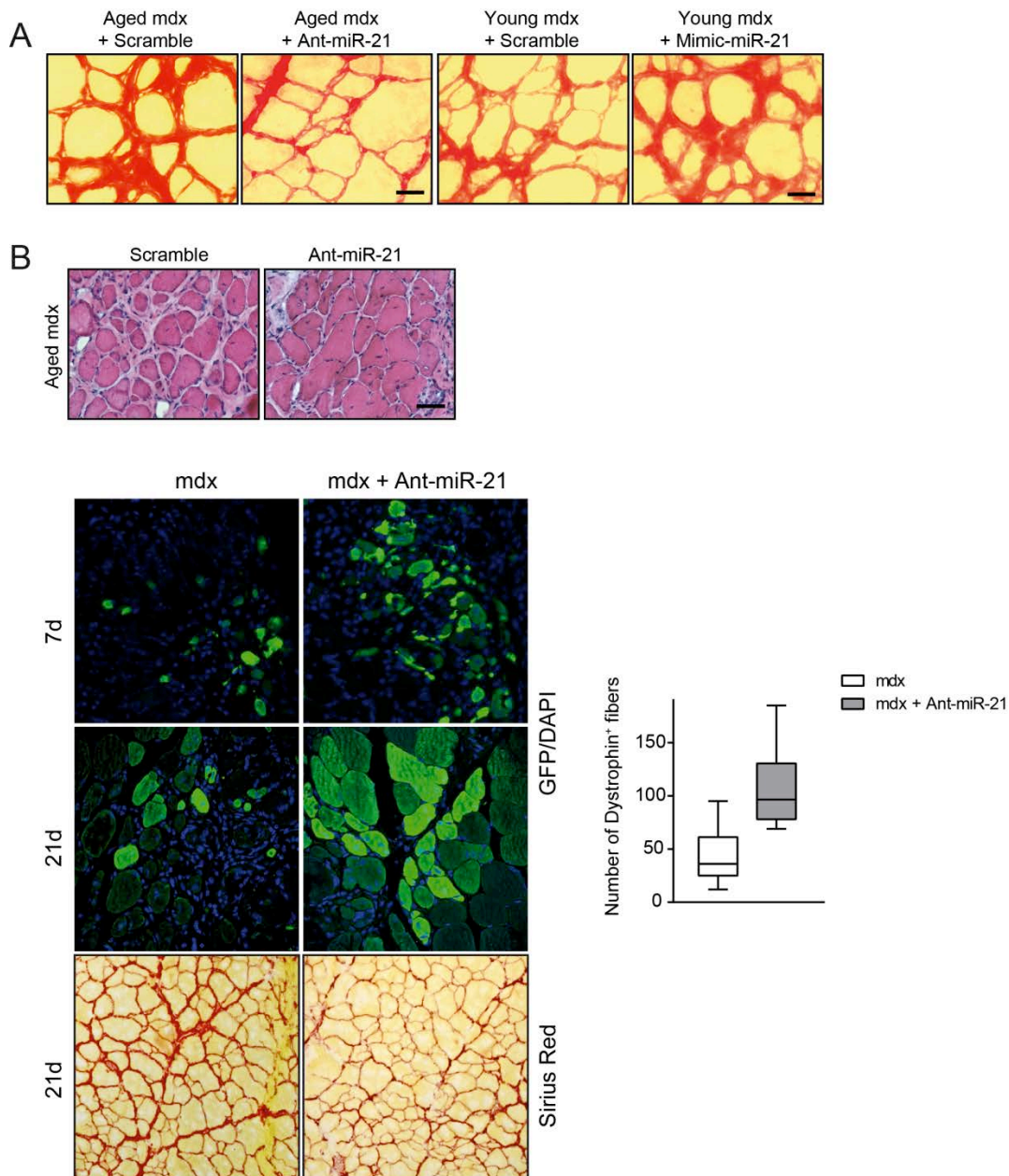


**Figure 5. A.** Sirius Red staining of gastrocnemius muscle sections from 24 month-old mdx mice, after administration of Ant-mir-21 (or Scramble) for 1 month; and from young mdx mice (3 months), after administration of Mimic-miR-21 (or Scramble). Scale bar: 25  $\mu$ m. **B.** H/E staining of gastrocnemius muscle sections from 24 month-old mdx mice treated with Ant-miR-21 (or Scramble) for 1 month. Scale bar: 50  $\mu$ m. **C.** Influence of the treatment with antago-miR-21 on the efficiency of engraftment of stem cells into dystrophic muscle. Mdx

mice pretreated with miR-21 inhibitor (Ant-miR-21) and control mdx mice (pretreated with a scramble miR) were injected equal numbers of satellite cells isolated by FACS from WT mice that were transduced with GFP lentivirus. After 7 or 21 days, muscles were immunostained for GFP. The number of GFP<sup>+</sup> fibers per muscle is shown. Bars depict mean values, and error bars represent SE.